UNIVERSIDAD DE CONCEPCIÓN

Centro de Investigación en Ingeniería Matemática (CI^{2}MA)

An a posteriori error estimator for the spectral fractional power of the Laplacian

Olga Barrera, Stéphane P. A. Bordas,
Raphaël Bulle, Franz Chouly,
Jack S. Hale

PREPRINT 2022-20

SERIE DE PRE-PUBLICACIONES

An a posteriori error estimator for the spectral fractional power of the Laplacian

Raphaël Bulle[1], Olga Barrera[4,5,6], Stéphane P. A. Bordas*[,1], Franz Chouly[2,3,7], and Jack S. Hale[1]

[1]Institute of Computational Engineering, University of Luxembourg, 6 Avenue de la Fonte, 4362 Esch-sur-Alzette, Luxembourg.
[2]Université Bourgogne Franche-Comté, Institut de Mathématiques de Bourgogne, 21078 Dijon, France.
[3]Center for Mathematical Modeling and Department of Mathematical Engineering, University of Chile and IRL 2807 – CNRS, Santiago, Chile.
[4]School of Engineering Computing and Mathematics, Oxford Brookes University, Oxford, UK.
[5]Department of Engineering Science, University of Oxford, Oxford, UK.
[6]Department of Medical Research,China Medical University Hospital, China Medical University, Taichung, Taiwan.
[7]Departamento de Ingeniería Matématica, CI²MA, Universidad de Concepción, Casilla 160-C, Concepción, Chile.

February 11, 2022

Abstract

We develop a novel a posteriori error estimator for the L^2 error committed by the finite element discretization of the solution of the fractional Laplacian. Our a posteriori error estimator takes advantage of the semi–discretization scheme using a rational approximation which allows to reformulate the fractional problem into a family of non–fractional parametric problems. The estimator involves applying the implicit Bank–Weiser error estimation strategy to each parametric non–fractional problem and reconstructing the fractional error through the same rational approximation used to compute the solution to the original fractional problem. We provide several numerical examples in both two and three-dimensions demonstrating the effectivity of our estimator for varying fractional powers and its ability to drive an adaptive mesh refinement strategy.

Keywords: Finite element methods, A posteriori error estimation, Fractional partial differential equations, Adaptive refinement methods, Bank–Weiser error estimator

2020 Mathematics Subject Classification: 65N15, 65N30

1 Introduction

Fractional partial differential equations (FPDEs) have gained in popularity during the last two decades and are now applied in a wide range of fields [72] such as anomalous diffusion [22, 41, 50, 55, 75], electromagnetism and geophysical electromagnetism [29, 83], phase fluids [9, 11, 54], porous media [11, 40, 20, 36], quasi-geostrophic flows [27] and spatial statistics [21, 71].

The main interest in fractional models lies in their ability to reproduce nonlocal behavior with a relatively small number of parameters [15, 39]. While this nonlocality can be interesting from a modeling perspective, it also constitutes an ongoing challenge for numerical methods since applying standard approaches naturally leads to large dense linear systems that are computationally intractable.

In the last decade various numerical methods have been derived in order to circumvent the main issues associated with the application of standard numerical methods to FPDEs, the two main ones being the non–locality leading to dense linear systems and, for some particular definitions of the fractional operator, the evaluation of singular integrals [6, 8].

We focus on discretization schemes based on finite element methods, other methods can be found e.g. in [1, 67, 78]. Among the methods addressing the above numerical issues, we can cite: methods

*Corresponding author: stephane.bordas@uni.lu

to efficiently solve eigenvalue problems [41], multigrid methods for performing efficient dense matrix–vector products [6, 8], hybrid finite element–spectral schemes [7], Dirichlet-to-Neumann maps (such as the Caffarelli–Silvestre extension) [13, 37, 45, 58, 75, 80], semigroups methods [46, 47, 79], rational approximation methods [2, 66, 68], Dunford–Taylor integrals [21, 23, 24, 26, 28, 31, 61, 68] (which can be considered as particular examples of rational approximation methods) and reduced basis methods [48, 49, 52].

Although we focus exclusively on the spectral definition of the fractional Laplacian, there is no unique definition of the fractional power of the Laplacian operator. The three most frequently found definitions of the fractional Laplacian are: the integral fractional Laplacian, defined from the principal value of a singular integral over the whole space $\mathbb{R}^d$ [6, 8, 25, 37, 51], the regional fractional Laplacian, defined by the same singular integral but over a bounded domain only [44, 55, 57, 74] and the spectral fractional Laplacian, defined from the spectrum of the standard Laplacian over a bounded domain [7, 14, 17, 46, 66, 73]. The different definitions are equivalent in the entire space $\mathbb{R}^d$, but this is no longer the case on a bounded domain [22, 55, 70, 72]. These definitions lead to significantly different mathematical problems associated with infinitesimal generators of different stochastic processes [72, 55].

Efficient methods for solving fractional problems typically rely on a combination of different discretization methods. For example, [28], which is also the foundation of this work, combines a quadrature scheme for the Dunford–Taylor integral representation of the spectral fractional Laplacian with a standard finite element method in space. Both the quadrature scheme and the finite element method induce discretization errors. Each of these schemes is associated with its own discretization error. In order to achieve a solution to a given accuracy while avoiding wasted computational time, these errors need to be balanced.

A priori error estimation has been tackled for some definitions of the fractional Laplacian, such as the integral Laplacian [5, 6, 7, 22, 28, 62] and the spectral fractional Laplacian [13, 14, 17, 28, 73, 75]. Unlike the standard Laplacian equation, solutions to the fractional Laplacian problems often exhibit strong boundary layers even for smooth data, particularly when the fractional power is low [63]. These singularities lead to computational difficulties and have to be taken into account using, for example a priori geometric mesh refinement towards the boundary of the domain [5, 18, 25, 31, 58], or partition of unity enrichments [30]. We emphasize that [28] contains already an a priori error analysis in the L^2 norm for the combined rational sum finite element method that we use in this work.

A posteriori error estimation has also been considered in the literature on fractional equations. A simple residual based estimator is proposed for the integral fractional Laplacian in [6]. A similar idea is used in the context of nonlocal variational inequalities in [62, 76]. Gradient-recovery based a posteriori error estimation has been developed in the context of fractional differential equations in [84]. In [22, 45] the authors present another estimator, based on the solution to local problems on cylindrical stars, for the integral fractional Laplacian discretized using the Caffarelli–Silvestre extension. A weighted residual estimator is derived in [59] in the same context.

To our knowledge, no a posteriori error estimation method has been derived for the spectral fractional Laplacian, discretized using the rational approximation approach of [28].

2 Contribution

The main contribution of this work is the derivation of a novel a posteriori error estimator for the combined rational finite element approximation of the spectral fractional Laplacian. It is a natural a posteriori counterpart to the a priori results developed in [28].

Our work starts with the quadrature rule for the Dunford–Taylor integral proposed in the seminal work [28]. This method, and other rational approximation–based discretization methods, decompose the original fractional problem into a set of independent parametric non–fractional problems. From this point we develop an associated set of independent non–fractional a posteriori error estimation problems. We compute the Bank–Weiser hierarchical estimators [19] of the error between each non–fractional parametric problem solution and its finite element discretization, then the fractional problem discretization error is estimated by the sum of the parametric contributions via the rational approximation.

Our method leads to a fully local and parallelizable solution technique for the spectral fractional Laplacian with computable L^2 error. Our method is valid for any finite element degree (however, for the sake of brevity we do not show results with higher degree finite elements) and for one, two and three dimensional problems [36].

We implement our method in DOLFINx [64], the new problem solving environment of the FEniCS Project [12]. A simple demonstration implementation is included in the supplementary material. We show numerical results demonstrating that the estimator can correctly reproduce the a priori convergence rates derived in [28].

Our newly developed error estimator is then used to steer an adaptive mesh refinement algorithm, resulting in improved convergence rates for small fractional powers and strong boundary layers.

3 Motivation

Given a fractional power s in $(0, 1)$ and a rational approximation $\mathcal{Q}_s^\kappa(\lambda)$ of the function λ^{-s}, it is possible to construct a semi-discrete approximation u_κ of the solution u to a fractional Laplace equation as a weighted sum of solutions $(u_l)_l$ to non–fractional parametric problems. Then, a fully discrete approximation of u is obtained by discretizing the parametric solutions $(u_l)_l$ using a finite element method.

An a posteriori error estimator is then computed as the weighted sum of the Bank–Weiser estimators of the error between each u_l and its finite element discretization. As we will see in the following, the resulting numerical scheme is simple and its implementation in code is straightforward. Furthermore it maintains the appealing embarrassingly parallel nature of rational approximation schemes [28, 61, 66].

We remark on why we have chosen to use the Bank–Weiser type error estimator, as opposed to one of the many other error estimation strategies, e.g. explicit residual, equilibrated fluxes, or recovery-type estimators (see [10, 43] and references therein). In the case of fractional powers of the Laplacian operator, the resulting set of parametric problems consists of singularly–perturbed reaction–diffusion equations. It has been proven in [82] that the Bank–Weiser estimator is robust with respect to the coefficients appearing in these parametric problems when the error is measured in the natural norm. To our knowledge, no such robustness, which our numerical experiments do indicate, has been established for the L^2-norm for the Bank–Weiser estimator. Nevertheless, our numerical experiments indicate that this does appear to be the case. Moreover, the Bank–Weiser estimator can be straightforwardly applied to higher-order finite element methods and higher-dimension problems. In addition, its computational stencil is highly local which is particularly appealing for three-dimensional problems see e.g. [36].

In this work we focus on error estimation in the L^2 norm, the estimation of the error in the 'natural' fractional norm is the topic of ongoing work. For simplicity, we only consider fractional powers of the Laplacian with homogeneous Dirichlet boundary conditions.

4 Problem statement

For any subset ω of $\overline{\Omega}$ we denote $L^2(\omega)$ the space of square integrable functions on ω and $(\cdot,\cdot)_\omega$ its usual inner product. Let $H^1(\omega)$ be the Sobolev space of functions with first order weak derivatives in $L^2(\omega)$. The space $H^1(\omega)$ is endowed with the usual inner product $(\nabla\cdot,\nabla\cdot)_{L^2(\omega)} + (\cdot,\cdot)_{L^2(\omega)}$. We will omit the dependence in ω in the subscripts when $\omega = \Omega$. We will make use of the notation $\partial v/\partial n := \nabla v \cdot n$ for the normal derivative of a smooth enough function v. We denote $H_0^1(\Omega)$ the subspace of functions in $H^1(\Omega)$ with a zero trace on Γ.

We consider the family of eigenfunctions $\{\psi_i\}_{i=1}^\infty \subset H_0^1(\Omega)$ of the standard Laplacian operator with uniform zero Dirichlet boundary condition on Ω as well as the corresponding family of eigenvalues $\{\lambda_i\}_{i=1}^\infty$. We assume the Laplacian eigenvalues are sorted in increasing order and we assume $\lambda_0 \in \mathbb{R}$ is a lower bound of the spectrum

$$\lambda_0 \leqslant \lambda_1 \leqslant \cdots \leqslant \lambda_i \leqslant \lambda_{i+1} \leqslant \cdots \tag{1}$$

The family $\{\psi_i\}_{i=1}^\infty$ is an orthonormal basis of $L^2(\Omega)$. For s in $(0, 1)$ we introduce the spectral fractional

Sobolev space $\mathbb{H}^s$ and its natural norm

$$\mathbb{H}^s := \left\{ v \in L^2(\Omega),\ \sum_{i=1}^{\infty} \lambda_i^s \left(v, \psi_i\right)^2 < \infty \right\}, \qquad \|v\|_{\mathbb{H}^s}^2 := \sum_{i=1}^{\infty} \lambda_i^s \left(v, \psi_i\right)^2. \tag{2}$$

Especially, for $0 \leqslant s \leqslant 1$ we have $H_0^1(\Omega) = \mathbb{H}^1(\Omega) \subseteq \mathbb{H}^s(\Omega) \subseteq L^2(\Omega) =: \mathbb{H}^0(\Omega)$ and the norm $\|\cdot\|_{\mathbb{H}^s}$ coincide with $\|\cdot\|_{L^2}$ when $s = 0$ and with $|\cdot|_{H^1}$ when $s = 1$.

4.1 The spectral fractional Laplacian

Let s be a real number in $(0, 1)$ and f be a given function in $L^2(\Omega)$. We consider the following fractional Laplacian problem: we look for a function u such that

$$(-\Delta)^s u = f \text{ in } \Omega, \quad u = 0 \text{ on } \Gamma. \tag{3}$$

The solution u of eq. (3) is defined using the spectrum of the standard Laplacian [14]

$$u := \sum_{i=1}^{\infty} \lambda_i^{-s} \left(f, \psi_i\right) \psi_i. \tag{4}$$

If we notice that

$$\left(u, \psi_i\right) = \lambda_i^{-s} \left(f, \psi_i\right), \qquad \forall i \geqslant 1, \tag{5}$$

then, for f in $L^2(\Omega)$ we can show that

$$\|u\|_{\mathbb{H}^{2s}} = \|f\|_{L^2}. \tag{6}$$

Moreover, we can derive an *equivalent* formulation of eq. (3). If we multiply eq. (3) by test functions v in $\mathbb{H}^s(\Omega)$ and integrate over Ω, we obtain

$$\int_\Omega (-\Delta)^s u v = \int_\Omega f v, \quad \forall v \in \mathbb{H}^s(\Omega). \tag{7}$$

Now, using the decompositions of u, v and f in the basis $(\psi_i)_{i=1}^{+\infty}$ we have

$$\left((-\Delta)^s u, v\right) = \sum_{i=1}^{\infty} \lambda_i^s u_i v_i = \sum_{i,j=1}^{\infty} \lambda_i^{s/2} u_i \lambda_j^{s/2} v_j \left(\psi_i, \psi_j\right) = \left((-\Delta)^{s/2} u, (-\Delta)^{s/2} v\right).$$

Then, the solution u to eq. (7) satisfies

$$\left((-\Delta)^{s/2} u, (-\Delta)^{s/2} v\right) = \left(f, v\right), \quad \forall v \in \mathbb{H}^s(\Omega). \tag{8}$$

Conversely, if u is solution to eq. (8), we can show eq. (5) which leads to eq. (4) and eq. (3).

4.2 Rational approximation

Our method relies on rational approximations of the real function $\lambda \mapsto \lambda^{-s}$ for s in $(0, 1)$ and $\lambda \geqslant \lambda_0$ for some fixed $\lambda_0 > 0$. We are particularly interested in an example provided in [28]. This example is based on the following expression derived from Euler's reflection formula

$$\lambda^{-s} = \frac{2 \sin(\pi s)}{\pi} \int_{-\infty}^{+\infty} \mathrm{e}^{2sy} \left(1 + \mathrm{e}^{2y} \lambda\right)^{-1} \ \mathrm{d}y. \tag{9}$$

Then, the rational approximation is obtained from eq. (9) by discretizing the integral on the right-hand side with a trapezoidal quadrature rule,

$$\lambda^{-s} \simeq \mathcal{Q}_s^\kappa(\lambda) := \frac{2 \sin(\pi s)}{\pi \kappa} \sum_{l=-M(\kappa)}^{N(\kappa)} \mathrm{e}^{2sl\kappa} \left(1 + \mathrm{e}^{2l\kappa} \lambda\right)^{-1}, \tag{10}$$

where $\kappa > 0$ is the fineness parameter and

$$M(\kappa) := \left\lceil \frac{\pi^2}{4s\kappa^2} \right\rceil, \quad \text{and} \quad N(\kappa) := \left\lceil \frac{\pi^2}{4(1-s)\kappa^2} \right\rceil, \tag{11}$$

where $\lceil \cdot \rceil$ is the ceiling function.

This particular scheme has some advantages compared to other rational methods. The coefficients $(\mathrm{e}^{2sl\kappa})_{l=-M}^{N}$ and $(\mathrm{e}^{2l\kappa})_{l=-M}^{N}$ are very easy to compute in comparison with methods based on e.g. best uniform rational approximations (BURA) (see [2, 66, 68, 69]). This scheme is also among the most efficient as shown in recent comparison studies (see [68, 81]). Various other examples of rational approximations can be found e.g. in [2, 3, 60, 66, 81]. We want to highlight again that the error estimation scheme developed later can be derived in the same manner regardless of the choice of the rational approximation, as long as it leads to a set of well–posed non–fractional parametric problems.

It has been shown in [28] that $\mathcal{Q}_s^\kappa$ converges uniformly to λ^{-s} at an exponential rate as $\kappa \to 0$. Especially, the approximation error is bounded by

$$\left|\lambda^{-s} - \mathcal{Q}_s^\kappa(\lambda)\right| \leqslant \varepsilon_s(\kappa), \qquad \forall \lambda \geqslant \lambda_0,\ \forall \kappa > 0, \tag{12}$$

with

$$\varepsilon_s(\kappa) = \frac{2\sin(\pi s)}{\pi} \left[\frac{1}{2s} + \frac{1}{2(1-s)\lambda_0}\right] \left[\frac{1}{1-\mathrm{e}^{-\pi^2/(2\kappa)}} + 1\right] \mathrm{e}^{-\pi^2/(2\kappa)}. \tag{13}$$

Asymptotically, $\varepsilon_s(\kappa)$ behaves like $\mathrm{e}^{-\pi^2/(2\kappa)}$ as $\kappa \to 0$.

5 Discretization

We combine the rational approximation eq. (10) with a finite element method to derive a fully discrete approximation of the solution u to eq. (8).

5.1 Rational semi-discrete approximation

From eq. (10) we can derive semi-discrete approximations of the solution u to eq. (8) by considering

$$u_\kappa := \frac{2\sin(\pi s)}{\pi\kappa} \sum_{l=-M(\kappa)}^{N(\kappa)} \mathrm{e}^{2sl\kappa}\, u_l, \tag{14}$$

where the functions $\{u_l\}_{l=1}^{N}$ are solutions to the parametric problems: for each l in $[\![-M, N]\!]$, find u_l in H_0^1 such that

$$(u_l, w) + \mathrm{e}^{2sl\kappa}\,(\nabla u_l, \nabla w) = (f, w) \quad \forall w \in H_0^1. \tag{15}$$

It has been proved in [28] that the semi-discrete approximation u_κ converges to u in $L^2(\Omega)$ at the same speed as $\mathcal{Q}_s^\kappa(\lambda)$ converges to λ^{-s}. More precisely,

$$\|u - u_\kappa\|_{L^2} \leqslant \varepsilon_s(\kappa)\|f\|_{L^2}, \qquad \forall \kappa > 0. \tag{16}$$

where $\varepsilon_s(\kappa)$ is defined in eq. (13).

We can deduce from eq. (16) the following two important points. Firstly, the rational approximation u_κ converges to u exponentially fast in κ. Therefore, it does not constitute a bottleneck in the rate of convergence when combined with a finite element method to obtain a fully discrete approximation. Secondly, the right-hand side of eq. (16) is technically an *a posteriori estimation* of the rational discretization error since $\varepsilon_s(\kappa)$ and $\|f\|_{L^2}$ can be calculated almost entirely using *a priori* known data. The only parameter that is not so easily computable in ε_s is λ_0, a lower bound of the spectrum of the Laplacian on Ω. The bound $\varepsilon_s(\kappa)$ can be optimized by taking $\lambda_0 = \lambda_1$ but given its exponential convergence rate, $\varepsilon_s(\kappa)$ will not drastically deteriorates if $\lambda_0 < \lambda_1$. Moreover, precise guaranteed lower bounds for λ_1 could be obtained following e.g. [38, 42].

5.2 Finite element discretization

In order to get a fully discrete approximation of u, we use a finite element method to discretize the parametric problems eq. (15). Although it is not mandatory, we use the same mesh and same finite element space for all the parametric problems. We discuss this choice, and possible alternative strategies, in section 7.

Let $\mathcal{T}$ be a mesh on the domain Ω, composed of cells $\mathcal{T} = \{T\}$, facets $\mathcal{E} = \{E\}$ (we call *facets* the edges in dimension two and the faces in dimension three), and vertices. The mesh $\mathcal{T}$ is supposed to be regular, in Ciarlet's sense: $h_T/\rho_T \leqslant \gamma,\ \forall T \in \mathcal{T}$, where h_T is the diameter of a cell T, ρ_T the diameter of its inscribed ball, and γ is a positive constant fixed once and for all. The subset of facets that are not coincident with the boundary Γ (called interior facets) is denoted $\mathcal{E}_I$. Let n^+ and n^- in $\mathbb{R}^d$ be the outward unit normals to a given edge as seen by two cells T^+ and T^- incident to a common edge E. The space of polynomials of order p on a cell T is denoted $\mathcal{P}_p(T)$ and the continuous Lagrange finite element space of order p on the mesh $\mathcal{T}$ is defined by

$$V^p := \left\{ v_p \in H^1(\Omega), v_{p|T} \in \mathcal{P}_p(T)\ \forall T \in \mathcal{T} \right\}. \tag{17}$$

We denote V_0^p the finite element space composed by functions of V^p vanishing on the boundary Γ. For a given index l, the finite element discretization of eq. (15) reads: for each l in $[\![-M, N]\!]$, find $u_{l,p}$ in V_0^p such that

$$(u_{l,p}, v_p) + \mathrm{e}^{2l\kappa} \left(\nabla u_{l,p}, \nabla v_p\right) = \left(f, v_p\right), \quad \forall v_p \in V_0^p. \tag{18}$$

Then, combining eq. (14) with eq. (18) we can give a fully discrete approximation of the solution to eq. (8)

$$u \approx u_{\kappa,p} := \frac{2\sin(\pi s)}{\pi\kappa} \sum_{l=-M(\kappa)}^{N(\kappa)} \mathrm{e}^{2sl\kappa}\, u_{l,p}. \tag{19}$$

The computation of $u_{\kappa,p}$ is summarized in the top part of fig. 1.

6 Finite element discretization error analysis

According to what we have seen in section 4.2, the rational approximation error, characterized by $\|u - u_\kappa\|_{L^2}$ converges exponentially fast. Consequently, we will consider this error to be negligible and assume that the rational scheme $\mathcal{Q}_s^\kappa$ is precise enough (i.e. κ is small enough) so that

$$u \simeq u_\kappa. \tag{20}$$

Our goal is to bound the discretization error in the L^2 norm

$$\|u - u_{\kappa,p}\|_{L^2} \simeq \|u_\kappa - u_{\kappa,p}\|_{L^2}. \tag{21}$$

Since for any $s \in (0,1)$, the discrepancy $u - u_{\kappa,p}$ belongs to $\mathbb{H}^s(\Omega) \subset L^2(\Omega)$, the error can be measured in the L^2 norm for any value of the fractional power s.

6.1 Heuristics

Let us start with some heuristics motivating the derivation of our a posteriori error estimator. The main idea is to derive a function $e^{\mathrm{bw}}_{\kappa,T}$ that locally represents the discretization error in the solution to the fractional problem $(u_\kappa - u_{\kappa,p})_{|T}$ on a cell T of the mesh. Thanks to the rational approximation we notice that

$$(u_\kappa - u_{\kappa,p})_{|T} = \frac{2\sin(\pi s)}{\pi\kappa} \sum_{l=-M}^{N} \mathrm{e}^{2sl\kappa} (u_l - u_{l,p})_{|T}. \tag{22}$$

So we can use the framework proposed by Bank and Weiser in [19] to derive solutions $e^{\mathrm{bw}}_{l,T}$ such that

$$e^{\mathrm{bw}}_{l,T} \simeq (u_l - u_{l,p})_{|T}, \quad \forall l \in [\![-M, N]\!],\ \forall T \in \mathcal{T}. \tag{23}$$

We obtain $e^{\mathrm{bw}}_{\kappa,T}$ using the rational approximation sum

$$e^{\mathrm{bw}}_{\kappa,T} := \frac{2\sin(\pi s)}{\pi\kappa} \sum_{l=-M}^{N} \mathrm{e}^{2sl\kappa}\, e^{\mathrm{bw}}_{l,T} \simeq (u_\kappa - u_{\kappa,p})_{|T}, \quad \forall T \in \mathcal{T}. \tag{24}$$

Finally, we can estimate the L^2 error on the cell T by taking the norm of the function $e^{\mathrm{bw}}_{\kappa,T}$

$$\|e^{\mathrm{bw}}_{\kappa,T}\|_{L^2} \approx \|u_\kappa - u_{\kappa,p}\|_{|T}. \tag{25}$$

These heuristics are summarized in fig. 1.

We would like to emphasize that the Bank–Weiser estimator is not the only possible choice. In fact, the Bank–Weiser estimator could be replaced with another estimator based on the solves of local problems, such as e.g. the one used in [75].

6.2 A posteriori error estimation

Let us now derive our a posteriori error estimation method more precisely. As mentioned in the last subsection, this estimator is based on a hierarchical estimator computed from the solves of local Neumann problems on the cells and introduced for the first time by Bank and Weiser in [19].

Let T be a cell of the mesh. We make use of the following local finite element spaces

$$V^p_T := \left\{ v_{p,T} \in \mathcal{P}_p(T),\ v_{p,T} = 0 \text{ in } (\Omega \setminus \overline{T}) \cup (\overline{T} \cap \partial\Omega) \right\}. \tag{26}$$

Let us now consider two non-negative integers p_+ and p_- such that $p_+ > p_- \geqslant 0$ and $\mathcal{L}_T : V^{p_+}_T \longrightarrow V^{p_-}_T$ the local Lagrange interpolation operator. We introduce the *local Bank–Weiser space*, defined by

$$V^{\mathrm{bw}}_T := \ker(\mathcal{L}_T) = \left\{ v_{p_+,T} \in V^{p_+}_T,\ \mathcal{L}_T(v_{p_+,T}) = 0 \right\}. \tag{27}$$

The local parametric Bank–Weiser problem associated to the parametric problems eq. (15) and eq. (18) reads

$$\int_T e^{\mathrm{bw}}_{l,T} v^{\mathrm{bw}}_T + \mathrm{e}^{2sl\kappa} \int_T \nabla e^{\mathrm{bw}}_{l,T} \cdot \nabla v^{\mathrm{bw}}_T = \int_T r_{l,T} v^{\mathrm{bw}}_T + \frac{1}{2} \sum_{E \in \partial T} \int_E J_{l,E} v^{\mathrm{bw}}_T,\ \forall v^{\mathrm{bw}}_T \in V^{\mathrm{bw}}_T \tag{28}$$

where $r_{l,T}$ and $J_{l,T}$ are defined as follow:

$$r_{l,T} := f_{|T} - u_{l,p\,|T} + \mathrm{e}^{2l\kappa}\, \Delta u_{l,p\,|T}, \quad \text{and} \quad J_{l,T} := \mathrm{e}^{2l\kappa} \left[\!\!\left[\frac{\partial u_{l,p}}{\partial n} \right]\!\!\right]_E. \tag{29}$$

The solution $e^{\mathrm{bw}}_{l,T}$ in V^{bw}_T is the local parametric Bank–Weiser solution. More details about the computation and implementation of the Bank–Weiser solutions can be found in [19, 36].

Then, we derive the local *fractional* Bank–Weiser solution by summing the local parametric Bank–Weiser solutions into the rational approximation sum

$$e^{\mathrm{bw}}_{\kappa,T} := \frac{2\sin(\pi s)}{\pi\kappa} \sum_{l=-M}^{N} \mathrm{e}^{2sl\kappa}\, e^{\mathrm{bw}}_{l,T}. \tag{30}$$

The local fractional Bank–Weiser estimator is then defined as the L^2 norm of this local solution

$$\eta^{\mathrm{bw}}_{\kappa,T} := \|e^{\mathrm{bw}}_{\kappa,T}\|_{L^2(T)}. \tag{31}$$

The global fractional Bank–Weiser estimator is then defined by

$$\eta^{\mathrm{bw}^2}_{\kappa} := \sum_{T \in \mathcal{T}} \eta^{\mathrm{bw}\ 2}_{\kappa,T}. \tag{32}$$

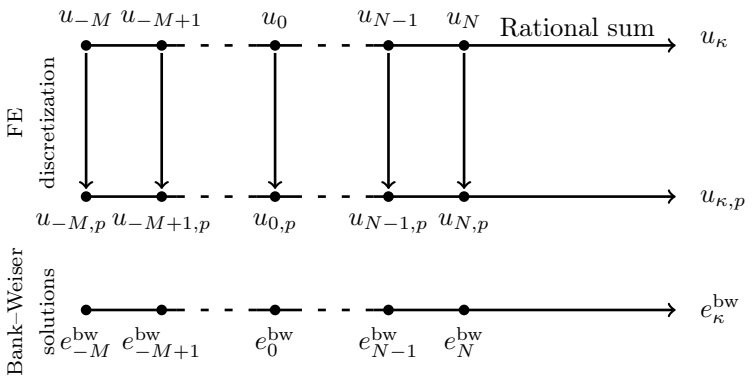

Figure 1: Summary of the computation of the fractional solution approximation and of the fractional Bank–Weiser solution.

7 Adaptive refinement

One of the main applications of a posteriori error estimation is to drive adaptive mesh refinement algorithms. When the error is unevenly spread across the mesh, refining uniformly is a waste of computational resources leading to suboptimal convergence rates in the number of degrees of freedom. This problem is compounded for computationally expensive problems like fractional problems. Moreover, it is known that fractional problems often show a boundary layer behavior, the discretization error is consequently large in a localized region near the boundary [4, 32, 81]. This problem has been tackled using graded meshes that are refined near the boundary based on a priori or a posteriori considerations [22, 45, 62, 73]. As expected, the use of graded meshes improves the convergence of the methods.

Adaptive refinement algorithms are based on the loop

$$\cdots \longrightarrow \text{Solve} \longrightarrow \text{Estimate} \longrightarrow \text{Mark} \longrightarrow \text{Refine} \longrightarrow \cdots$$

In this work we are concerned with developments in the modules *solve* and *estimate*. We are using totally standard approaches, namely the Dörfler algorithm [53] for the *mark* module and the Plaza–Carey algorithm [77] for the *refine* module.

Rational approximation methods have the advantage of being fully parallelizable due to the independence of the parametric problems from each other. Similarly, the local a posteriori error estimation method we have presented earlier is also parallelizable since the computation of the local Bank–Weiser solutions on the cells are independent from each other. Our error estimation strategy combines these advantages and is fully parallelizable both with respect to the parametric problems and local estimators computation. An example of error estimation and adaptive refinement algorithm based on our method is shown in fig. 2.

The algorithm presented in fig. 2 is based on three loops: one **While** loop and two **For** loops. The **While** loop is due to the adaptive refinement procedure and can not be parallelized. However, the two **For** loops are fully parallelizable and this parallelization can be highly advantageous for large three-dimensional problems.

Note that there is no guarantee that the mesh we obtain at the end of the main **While** loop in fig. 2 is optimal for all the parametric problems. For some of the parametric solutions without boundary layers the mesh is certainly over-refined. An alternative approach could be to compute the L^2 norms of the parametric Bank–Weiser solutions $e^{\mathrm{bw}}_{l,T}$ in order to derive parametric Bank–Weiser estimators and refine the meshes independently for each parametric problem. This would require the storage of a possibly different mesh for each parametric problem at each iteration. More importantly, this would mean summing parametric finite element solutions coming from different and possibly non-nested meshes. Properly addressing this question is beyond the scope of this study. Nonetheless, we give some hints the numerical section section 9.1.

Choose a tolerance $\varepsilon > 0$
Choose an initial mesh $\mathcal{T}_{n=0}$
Choose κ such that $\varepsilon_s(\kappa)\|f\|_{L^2} < \varepsilon$
Generate the rational approximation $\mathcal{Q}_s^\kappa$ coefficients
Initialize the estimator $\eta_\kappa^{\mathrm{bw}} = \varepsilon + 1$

While $\eta_\kappa^{\mathrm{bw}} > \varepsilon$:

Initialize the local Bank–Weiser solutions $\{e_{\kappa,T}^{\mathrm{bw}}\}_T$ to zero
Initialize the solution $u_{\kappa,p}$ to zero

For each parametric problem $l \in [\![-M, N]\!]$:

Solve eq. (18) on $\mathcal{T}_n$ to obtain $u_{l,p}$
Add $(2\sin(\pi s)/\pi s)\,\mathrm{e}^{2sl\kappa}\,u_{l,p}$ to $u_{\kappa,p}$

For each cell T of $\mathcal{T}_n$:

Solve eq. (28) to obtain $e_{l,T}^{\mathrm{bw}}$
Add $(2\sin(\pi s)/\pi s)\,\mathrm{e}^{2sl\kappa}\,e_{l,T}^{\mathrm{bw}}$ to $e_{\kappa,T}^{\mathrm{bw}}$

Compute the L^2 norms of $\{e_{\kappa,T}^{\mathrm{bw}}\}_T$ to obtain $\{\eta_{\kappa,T}^{\mathrm{bw}}\}_T$
Take the square root of the sum of $\{{\eta_{\kappa,T}^{\mathrm{bw}}}^2\}_T$ to obtain $\eta_\kappa^{\mathrm{bw}}$

If $\eta_\kappa^{\mathrm{bw}} \leqslant \varepsilon$:

Stop the loop
Return $u_{\kappa,p}$ and $\eta_\kappa^{\mathrm{bw}}$

Mark the mesh using $\{\eta_{\kappa,T}^{\mathrm{bw}}\}_T$
Refine the mesh and replace $\mathcal{T}_n$ by $\mathcal{T}_{n+1}$

Figure 2: Error estimation and adaptive refinement algorithm outline in pseudo–code.

Frac. power	0.1	0.3	0.5	0.7	0.9
Num. param. prob.	408	176	149	176	408

Table 1: Number of parametric problems solved for each fractional power.

8 Implementation

We have implemented our method using the DOLFINX finite element solver of the FEniCS Project [12]. Each parametric subproblem is submitted to a batch job queue. A distinct MPI communicator is used for each job. We use a standard first-order Lagrange finite element method and the resulting linear system is solved using the conjugate gradient method preconditioned using BoomerAMG from HYPRE [56] via the interface in PETSc [16]. To compute the Bank-Weiser error estimator for each subproblem we use the methodology outlined in [36] and implemented in the FEniCSx-EE package [35]. For every subproblem the computed solution and error estimate is written to disk in HDF5 format. A final step, running on a single MPI communicator, reads the solutions and error estimates for all subproblems, computes the quadrature sums using `axpy` operations, defines the marked set of cells to be refined using the Dörfler algorithm [53], and finally refines the mesh using the Plaza–Carey algorithm [77].

A more complex implementation using a single MPI communicator split into sub-communicators would remove the necessity of reading and writing the solution and error estimate for each subproblem to and from disk. However, in practice the cost of computing the parametric solutions massively dominates all other costs.

9 Numerical results

First, we need to choose the value of κ in order to guarantee that the rational approximation error is negligible. From eq. (16), we know a bound that depends on s, λ_0 and $\|f\|_{L^2}$. However, in all our test cases we know that $\lambda_0 = \lambda_1 = 1$ is a lower bound for the spectrum of the Laplacian and the data f is always chosen such that $\|f\|_{L^2} = 1$. It turns out that taking $\kappa = 0.26$ ensures that $\|u - u_\kappa\|_{L^2} \leqslant 10^{-8}$, no matter the choice of $s \in (0, 1)$. This choice leads to a different number of parametric problems to solve for each fractional power, these numbers are detailed in table 1.

When analytical solutions are known, we provide the efficiency indices of the Bank–Weiser estimator, defined by $\eta_\kappa^{\mathrm{bw}} / \|u_\kappa - u_{\kappa,1}\|_{L^2}$.

9.1 Two-dimensional product of sines test case

We solve eq. (3) on the square $\Omega = (0, \pi)^2$ with data $f(x, y) = (2/\pi)\sin(x)\sin(y)$. The analytical solution to this problem is given by $u(x, y) = 2^{-s}(2/\pi)\sin(x)\sin(y)$. Moreover, the analytical solutions to the parametric problems eq. (15) are also known $u_l(x, y) = (1 + 2\,\mathrm{e}^{2l\kappa})^{-1}(2/\pi)\sin(x)\sin(y)$. The problem is solved on a hierarchy of structured (triangular) meshes. For this test case the solution u shows no boundary layer behavior, therefore adaptive refinement cannot improve the convergence rate. Consequently we only perform uniform refinement on this case. As we can see on fig. 3, the Bank–Weiser estimator tends to be very accurate when the mesh is fine enough when $s = 0.3$ and $s = 0.7$. In fact, its accuracy is robust with respect to the fractional power. The efficiency indices are computed by taking the average of the ratios for the five last meshes of the hierarchy and are shown for various fractional powers in table 3.

Theorem 4.3 from [28] gives a convergence rate for the finite element scheme depending on the elliptic regularity index α of the Laplacian over Ω, on the fractional power and on the regularity index δ of the data f. Since Ω is convex the elliptic "pick-up" regularity index α can be taken to be 1 [22] and since f is infinitely smooth the coefficient δ can be taken as large as wanted. Consequently, Theorem 4.3 in [28] predicts a convergence rate of dof^{-1} for this test case. The convergence rates we measure in practice, shown in table 2, are coherent with this prediction. These rates are computed from a linear regression fit on the values obtained on the five last meshes of the hierarchy.

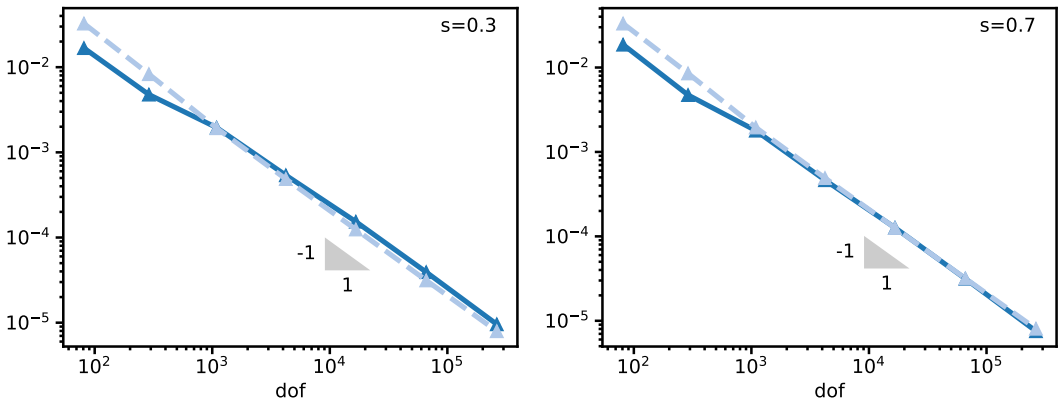

Figure 3: **Two-dimensional product of sines test case:** the Bank–Weiser estimator $\eta_\kappa^{\mathrm{bw}}$ in solid blue line is compared to the exact error in dashed light blue line for $s = 0.3$ and $s = 0.7$.

9.1.1 Parametric problems discretization error

Since we know the analytical solutions to the parametric problems in this case, it is possible to compute the exact parametric discretization errors $\|u_l - u_{l,1}\|_{L^2}$, for each $l \in [\![-M, N]\!]$. It is possible then to investigate the consequences of using the same mesh for all the parametric problems. In fig. 4 we have plotted the exact parametric errors after five steps of (uniform) refinement. As we can notice, the same mesh leads to a wide range of parametric errors values, especially for fractional powers s close to 1. These errors are particularly low for high values of the index l, when the diffusion part of the operator is dominant. However, when l becomes less than zero, i.e. when the reaction part is dominant the mesh seems to have an equal effect on the parametric errors. As expected these results suggest that the method can be optimized by using different meshes depending on l. In particular, coarser meshes would be sufficient for high values of l. These results are obtained for uniform refinement, further investigations deserve to be carried out for adaptive refinement.

As we explained earlier, using a different hierarchy of meshes for each parametric problem may be computationally advantageous, at the expense of ease of implementation. Several hierarchies of meshes would need to be stored and, in the case of adaptive mesh refinement, interpolation between possibly non-nested meshes would be required in order to compute the fractional solution u. To avoid these complications when adaptive refinement is used, we propose the following:

1. use the same hierarchy of meshes for all the parametric problems but not the same mesh. Some parametric problems might be solved on coarser meshes from the hierarchy and others on finer ones. This would allow to keep only one hierarchy of meshes stored in memory. Moreover, it would avoid the interpolation between non-nested meshes, since meshes from the same hierarchy being always nested.

2. selectively refine the mesh hierarchy: estimate the error globally for each parametric problem (this can be done using the local parametric Bank–Weiser solutions) and mark the parametric problems for which a finer mesh is required, using e.g. a marking algorithm similar to Dörfler's marking strategy.

9.2 Three-dimensional product of sines test case

This test case is the three-dimensional equivalent of the last test case. We solve eq. (3) on the cube $\Omega = (0, \pi)^3$ with data $f(x, y, z) = (2/\pi)^{3/2} \sin(x) \sin(y) \sin(z)$. The analytical solution to this problem is given by $u(x, y, z) = 3^{-s}(2/\pi)^{3/2} \sin(x) \sin(y) \sin(z)$. The problem is solved on a hierarchy of uniformly refined Cartesian (tetrahedral) meshes. As for the two-dimensional case, the solution u shows no boundary layer behavior and adaptive refinement is not required. For the same reasons as for

Frac. power	0.1	0.3	0.5	0.7	0.9
Estimator	-0.92	-0.97	-0.99	-1.00	-1.00
Exact error	-1.00	-1.00	-1.00	-1.00	-0.94

Table 2: **Two-dimensional product of sines test case:** convergence rates of the Bank–Weiser estimator and of the exact error for various fractional powers.

Frac. power	0.1	0.3	0.5	0.7	0.9
Est. eff. index	0.86	1.16	1.08	0.96	0.78

Table 3: **Two-dimensional product of sines test case:** efficiency indices of the Bank–Weiser estimator for various fractional powers.

the two-dimensional case, Theorem 4.3 from [28] predicts a convergence rate of $\mathrm{dof}^{-2/3}$ for the finite element scheme. fig. 5 shows the values of the Bank–Weiser estimator and of the exact error (computed from the knowledge of the analytical solution) for $s = 0.3$ and $s = 0.7$. As in the two-dimensional case, the efficiency indices are relatively robust with respect to the fractional powers. They are shown for various fractional powers in table 5 and are computed by taking the average of the indices from the three last meshes of the hierarchy. As we can see, the Bank–Weiser estimator efficiency indices for this three-dimensional case are not as good as in the two-dimensional case. We have already observed this behavior for non-fractional problems [34]. We can notice that the convergence rates, given in table 4, are coherent with the predictions of Theorem 4.3 from [28]. The convergence rates are computed from a linear regression on the values computed from the three last meshes of the hierarchy.

9.3 Two-dimensional checkerboard test case

We solve the problem introduced in the numerical results of [28]. We consider a unit square $\Omega = (0,1)^2$ with data $f : \Omega \to \mathbb{R}$ given for all $(x_1, x_2) \in \Omega$ by

$$f(x_1, x_2) = \begin{cases} 1, & \text{if } (x_1 - 0.5)(x_2 - 0.5) > 0, \\ 0, & \text{otherwise.} \end{cases} \tag{33}$$

The data $f \in \mathbb{H}^{1/2-\varepsilon}(\Omega)$ for all $\varepsilon > 0$. So in Theorem 4.3 of [28] the index $\delta < 1/2$ and since Ω is convex again α can be chosen equal to 1. Then, the predicted convergence rate (for uniform refinement) is $\ln(\sqrt{\mathrm{dof}})\mathrm{dof}^{-\beta}$ with

$$\beta = \begin{cases} 1, & \text{if } s > \frac{3}{4}, \\ s + \frac{1}{4}, & \text{otherwise.} \end{cases} \tag{34}$$

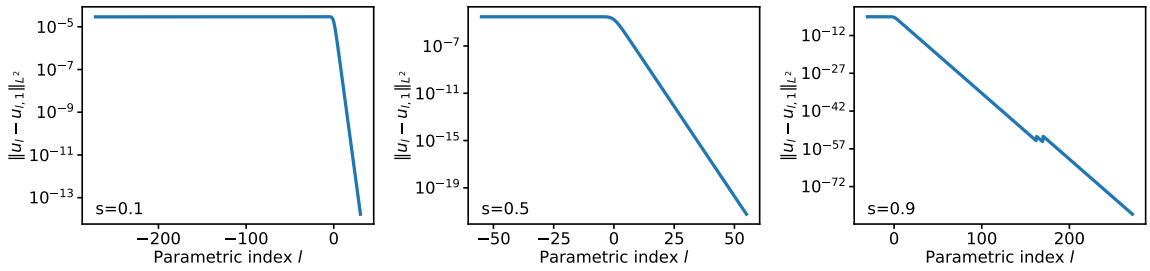

Figure 4: **Two-dimensional product of sines text case:** variation of the exact parametric errors with respect to the index $l \in [\![-M, N]\!]$ for three different fractional powers.

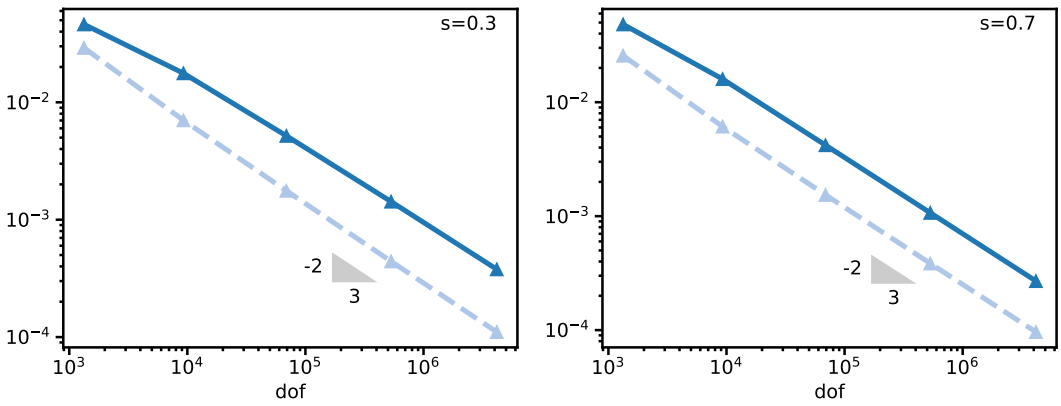

Figure 5: **Three-dimensional product of sines test case:** the Bank–Weiser estimator $\eta_\kappa^{\mathrm{bw}}$ in solid blue line is compared to the exact error in dashed light blue line for various fractional powers.

Frac. power	0.1	0.3	0.5	0.7	0.9
Estimator	-0.56	-0.60	-0.63	-0.65	-0.66
Exact error	-0.69	-0.69	-0.69	-0.69	-0.69

Table 4: **Three-dimensional product of sines test case:** convergence rates of the Bank–Weiser estimator and of the exact error for various fractional powers.

Frac. power	0.1	0.3	0.5	0.7	0.9
Est. eff. index	2.12	3.20	3.08	2.77	2.45

Table 5: **Three-dimensional product of sines test case:** efficiency indices of the Bank–Weiser estimator for various fractional powers.

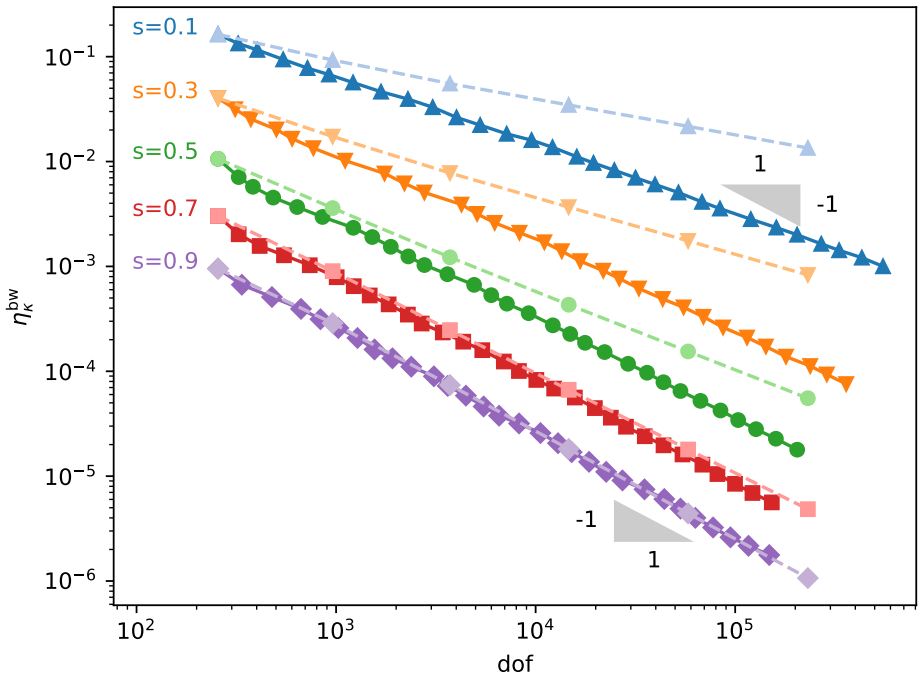

Figure 6: **Two-dimensional checkerboard test case:** for each fractional power we compare the values of the Bank–Weiser estimator $\eta_\kappa^{\mathrm{bw}}$ when uniform refinement is performed (dashed light lines) and when adaptive refinement is performed (solid lines).

Frac. power	0.1	0.3	0.5	0.7	0.9
Theory [28]	-0.35	-0.55	-0.75	-0.95	-1.00
Est. (unif.)	-0.35	-0.55	-0.76	-0.95	-1.00
Est. (adapt.)	-0.65	-0.84	-0.93	-0.97	-1.01

Table 6: **Two-dimensional checkerboard test case:** convergence slopes of the Bank–Weiser estimator for uniform refinement and for adaptive refinement compared to the values predicted by [28] for various fractional powers.

The predicted (if we omit the logarithmic term) and calculated convergence rates for different choices of s are given in table 6. As we can see on this table, the convergence rates for the Bank–Weiser estimator is globally coherent with the predictions. fig. 6 shows that adaptive refinement improves the convergence rate for small fractional powers. This is expected, the deterioration in the convergence rate is due to the boundary layer behavior of the solution that is getting stronger as the fractional power decreases. When the fractional power is close to 1, the solution behaves like the solution to a non-fractional problem for which adaptive refinement is no longer needed. This can be seen on fig. 7, after 10 steps of adaptive refinement, the mesh associated to fractional power $s = 0.9$ is almost uniformly refined while the meshes associated to $s = 0.5$ and $s = 0.1$ show strongly localized refinement. This explains why in fig. 6 we barely see any improvement in the convergence rate when the mesh is adaptively refined compared to uniformly refined when $s \geqslant 0.7$.

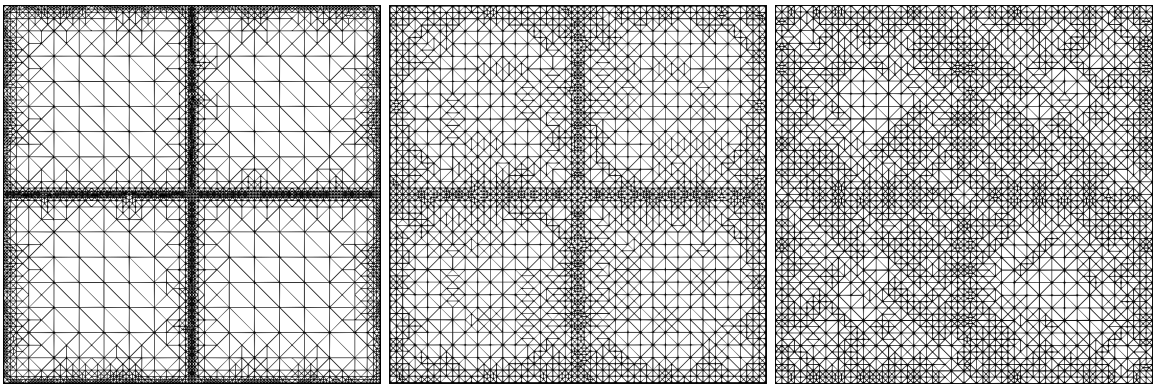

Figure 7: **Two-dimensional checkerboard test case:** meshes obtained after 10 steps of adaptive refinement steered by the Bank–Weiser estimator for $s = 0.1$, $s = 0.5$ and $s = 0.9$ from left to right.

Frac. power	0.1	0.3	0.5	0.7	0.9
Theory [28]	-0.23	-0.37	-0.50	-0.63	-0.67
Est. (unif.)	-0.24	-0.38	-0.52	-0.62	-0.67
Est. (adapt.)	-0.33	-0.46	-0.55	-0.65	-0.68

Table 7: **Three-dimensional checkerboard test case:** convergence slopes of the Bank–Weiser estimator for uniform refinement and for adaptive refinement compared to the values predicted by [28] for various fractional powers.

9.4 Three-dimensional checkerboard test case

This test case is the three-dimensional version of the above checkerboard problem. We solve eq. (3) on the unit cube $\Omega = (0,1)^3$, with data f such that

$$f(x_1,x_2,x_3) = \begin{cases} 1, & \text{if } (x_1-0.5)(x_2-0.5) > 0 \text{ and } (x_3-0.5) < 0, \\ 1, & \text{if } (x_1-0.5)(x_2-0.5) < 0 \text{ and } (x_3-0.5) > 0, \\ -1, & \text{otherwise.} \end{cases} \tag{35}$$

The finite element solution u_1 and the corresponding mesh after six steps of adaptive refinement are shown in fig. 8 for the fractional power $s = 0.5$. As for the two-dimensional case, $f \in \mathbb{H}^{1/2-\varepsilon}(\Omega)$ for all $\varepsilon > 0$. Consequently, once again Theorem 4.3 of [28] predicts a convergence rate (for uniform refinement) equal to $\ln\left(\mathrm{dof}^{1/3}\right)\mathrm{dof}^{-2\beta/3}$ with β given by eq. (34).

Once again, if we omit the logarithmic term, the predicted and calculated convergence rates are given in table 7. As in the two-dimensional case, the convergence rates of the Bank–Weiser estimator are globally coherent with the predictions and the boundary layer behavior becomes stronger as the fractional power decreases leading to poorer convergence rates. section 9.4 shows the values of the Bank–Weiser estimator for uniform and adaptive refinement and for several fractional powers.

10 Concluding remarks

In this work we presented a novel a posteriori error estimation method for the spectral fractional Laplacian. This method benefits from the embarrassingly parallel character of both the Bank–Weiser error estimator and the rational approximation methods, thus keeping the appealing computational aspects of the underlying methodology in [28]. Here are two important points we want to make to conclude this paper. First, the Bank–Weiser estimator seems to be equivalent to the L^2 exact error at least when structured meshes are used and when the solution u is smooth. Second, adaptive

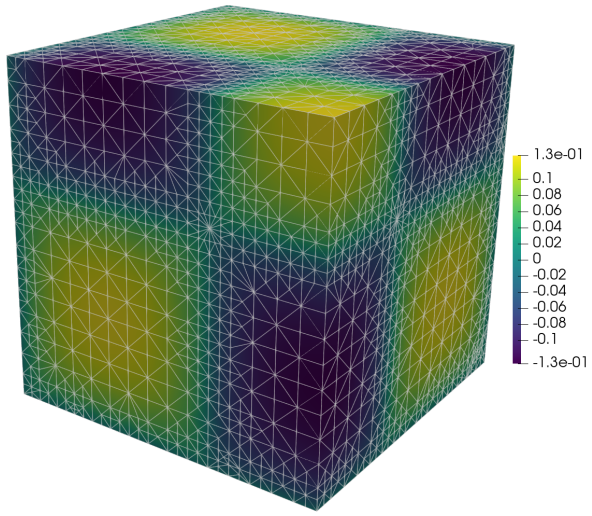

Figure 8: **Three-dimensional checkerboard test case:** finite element solution and mesh after six steps of adaptive refinement when $s = 0.5$. The unit cube domain $(0,1)^3$ is truncated by the three planes passing through the point $(0.25, 0.25, 0.25)$ and orthogonal to the vectors $(1,0,0)$, $(0,1,0)$ and $(0,0,1)$ respectively.

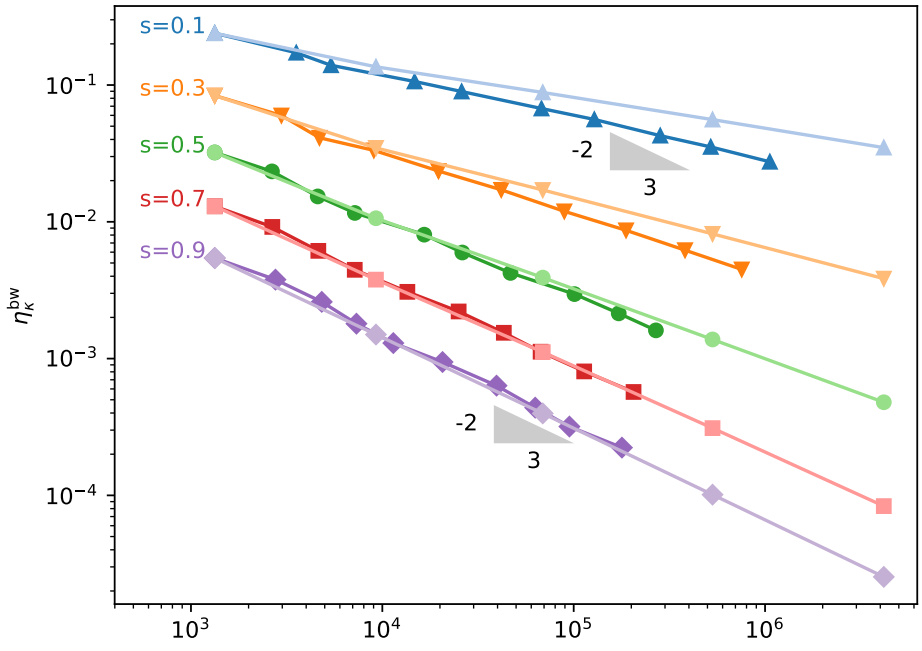

Figure 9: **Three-dimensional checkerboard test case:** for each fractional power we compare the values of the Bank–Weiser estimator $\eta_\kappa^{\mathrm{bw}}$ when uniform refinement is performed (dashed light lines) and when adaptive refinement is performed (solid lines).

refinement methods drastically improves the convergence rate compared to uniform refinement for fractional powers close to 0.

Finally, we give some future directions that we think are worth considering. More numerical tests could be performed, especially for higher order elements and/or using variants of the Bank–Weiser error estimator as considered in [36].

We would like also to study the derivation of an algorithm that allows to use different meshes to discretize the parametric problems in order to save computational time, as explained in section 9.1.1. The a posteriori error estimation of the error in the "natural" norm of the problem i.e. the spectral fractional norm defined in eq. (2) is another extension of this work that is worth to consider. The replacement of the Bank–Weiser estimator by an anisotropic a posteriori error estimator would improve the convergence rate even further in case of boundary layers, see e.g. [17, 58], Another interesting extension would be to test our method on fractional powers of other kinds of elliptic operators, following [28], on another definition of the fractional Laplacian operator [25] and/or other boundary conditions, following [14].

Supplementary material

A minimal example of adaptive finite element method for the two–dimensional spectral fractional Laplacian can be found in the following FEniCSx–Error–Estimation repository `https://github.com/jhale/fenicsx-error-estimation`. This minimal example code (LGPLv3) is also archived at `https://doi.org/10.6084/m9.figshare.19086695.v3`. A Docker image [65] is provided in which this code can be executed.

Acknowledgments

R.B. would like to acknowledge the support of the ASSIST research project of the University of Luxembourg. This publication has been prepared in the framework of the DRIVEN TWINNING project funded by the European Union's Horizon 2020 Research and Innovation programme under Grant Agreement No. 811099. F.C.'s work is partially supported by the I-Site BFC project NAANoD and the EIPHI Graduate School (contract ANR-17-EURE-0002).

References

[1] Lidia Aceto, Daniele Bertaccini, Fabio Durastante, and Paolo Novati. Rational Krylov methods for functions of matrices with applications to fractional partial differential equations. *J. Comput. Phys.*, 396:470–482, nov 2019. `doi:10.1016/j.jcp.2019.07.009`.

[2] Lidia Aceto and Paolo Novati. Rational Approximation to the Fractional Laplacian Operator in Reaction-Diffusion Problems. *SIAM J. Sci. Comput.*, 39(1):A214–A228, jan 2017. `arXiv:1607.04166`, `doi:10.1137/16M1064714`.

[3] Lidia Aceto and Paolo Novati. Rational approximations to fractional powers of self-adjoint positive operators. *Numer. Math.*, 143(1):1–16, sep 2019. `arXiv:1807.10086`, `doi:10.1007/s00211-019-01048-4`.

[4] Gabriel Acosta, Francisco M Bersetche, and Juan Pablo Borthagaray. A short FE implementation for a 2d homogeneous Dirichlet problem of a fractional Laplacian. *Comput. Math. with Appl.*, 74(4):784–816, aug 2017. `arXiv:1610.05558`, `doi:10.1016/j.camwa.2017.05.026`.

[5] Gabriel Acosta and Juan Pablo Borthagaray. A Fractional Laplace Equation: Regularity of Solutions and Finite Element Approximations. *SIAM J. Numer. Anal.*, 55(2):472–495, jan 2017. `arXiv:1507.08970`, `doi:10.1137/15M1033952`.

[6] Mark Ainsworth and Christian Glusa. Aspects of an adaptive finite element method for the fractional Laplacian: A priori and a posteriori error estimates, efficient implementation and multigrid solver. *Comput. Methods Appl. Mech. Eng.*, 327:4–35, dec 2017. arXiv:1708.03912, doi:10.1016/j.cma.2017.08.019.

[7] Mark Ainsworth and Christian Glusa. Hybrid Finite Element–Spectral Method for the Fractional Laplacian: Approximation Theory and Efficient Solver. *SIAM J. Sci. Comput.*, 40(4):A2383–A2405, jan 2018. URL: https://epubs.siam.org/doi/10.1137/17M1144696, arXiv:1709.01639, doi:10.1137/17M1144696.

[8] Mark Ainsworth and Christian Glusa. Towards an Efficient Finite Element Method for the Integral Fractional Laplacian on Polygonal Domains. *Contemp. Comput. Math. - A Celebr. 80th Birthd. Ian Sloan*, 40:17–57, 2018. arXiv:1708.01923, doi:10.1007/978-3-319-72456-0_2.

[9] Mark Ainsworth and Zhiping Mao. Analysis and Approximation of a Fractional Cahn–Hilliard Equation. *SIAM J. Numer. Anal.*, 55(4):1689–1718, jan 2017. doi:10.1137/16M1075302.

[10] Mark Ainsworth and J Tinsley Oden. *A Posteriori Error Estimation in Finite Element Analysis*. Pure and Applied Mathematics (New York). John Wiley & Sons, Inc., Hoboken, NJ, USA, aug 2000. doi:10.1002/9781118032824.

[11] Goro Akagi, Giulio Schimperna, and Antonio Segatti. Fractional Cahn–Hilliard, Allen–Cahn and porous medium equations. *J. Differ. Equ.*, 261(6):2935–2985, sep 2016. arXiv:1502.06383, doi:10.1016/j.jde.2016.05.016.

[12] Martin S Alnæs, Jan Blechta, Johan Hake, August Johansson, Benjamin Kehlet, Anders Logg, Chris Richardson, Johannes Ring, Marie E Rognes, and Garth N Wells. The FEniCS Project Version 1.5. *Arch. Numer. Softw.*, 2015. doi:10.11588/ans.2015.100.20553.

[13] Harbir Antil and Enrique Otárola. A FEM for an Optimal Control Problem of Fractional Powers of Elliptic Operators. *SIAM J. Control Optim.*, 53(6):3432–3456, jan 2015. arXiv:1406.7460, doi:10.1137/140975061.

[14] Harbir Antil, Johannes Pfefferer, and Sergejs Rogovs. Fractional operators with inhomogeneous boundary conditions: analysis, control, and discretization. *Commun. Math. Sci.*, 16(5):1395–1426, 2018. arXiv:1703.05256, doi:10.4310/CMS.2018.v16.n5.a11.

[15] Abdon Atangana. Fractional Operators and Their Applications. In *Fract. Oper. with Constant Var. Order with Appl. to Geo-Hydrology*, pages 79–112. Elsevier, 2018. doi:10.1016/B978-0-12-809670-3.00005-9.

[16] Satish Balay, Shrirang Abhyankar, Mark F Adams, Jed Brown, Peter Brune, Kris Buschelman, Lisandro Dalcin, Victor Eijkhout, William D Gropp, Dinesh Kaushik, Matthew G Knepley, Lois Curfman McInnes, Karl Rupp, Barry F Smith, Stefano Zampini, Hong Zhang, and Hong Zhang. PETSc Users Manual. Technical Report ANL-95/11 - Revision 3.7, Argonne National Laboratory, 2016. URL: http://www.mcs.anl.gov/petsc.

[17] Lehel Banjai, Jens M Melenk, Ricardo H Nochetto, Enrique Otárola, Abner J Salgado, and Christoph Schwab. Tensor FEM for Spectral Fractional Diffusion. *Found. Comput. Math.*, 19(4):901–962, aug 2019. arXiv:1707.07367, doi:10.1007/s10208-018-9402-3.

[18] Lehel Banjai, Jens M Melenk, and Christoph Schwab. Exponential convergence of hp FEM for spectral fractional diffusion in polygons. *arXiv*, pages 1–37, 2020. arXiv:2011.05701.

[19] Randolph E Bank and Alan Weiser. Some A Posteriori Error Estimators for Elliptic Partial Differential Equations. *Math. Comput.*, 44(170):283, apr 1985. doi:10.2307/2007953.

[20] O Barrera. A unified modelling and simulation for coupled anomalous transport in porous media and its finite element implementation. *Computational Mechanics*, pages 1–16, 2021.

[21] David Bolin, Kristin Kirchner, and Mihály Kovács. Numerical solution of fractional elliptic stochastic PDEs with spatial white noise. *IMA J. Numer. Anal.*, 40(2):1051–1073, apr 2020. arXiv:1705.06565, doi:10.1093/imanum/dry091.

[22] Andrea Bonito, Juan Pablo Borthagaray, Ricardo H Nochetto, Enrique Otárola, and Abner J Salgado. Numerical methods for fractional diffusion. *Comput. Vis. Sci.*, 19(5-6):19–46, dec 2018. arXiv:1707.01566, doi:10.1007/s00791-018-0289-y.

[23] Andrea Bonito, Wenyu Lei, and Joseph E Pasciak. Numerical Approximation of Space-Time Fractional Parabolic Equations. *Comput. Methods Appl. Math.*, 17(4):679–705, oct 2017. arXiv:1704.04254, doi:10.1515/cmam-2017-0032.

[24] Andrea Bonito, Wenyu Lei, and Joseph E Pasciak. The approximation of parabolic equations involving fractional powers of elliptic operators. *J. Comput. Appl. Math.*, 315:32–48, may 2017. arXiv:1607.07832, doi:10.1016/j.cam.2016.10.016.

[25] Andrea Bonito, Wenyu Lei, and Joseph E Pasciak. Numerical approximation of the integral fractional Laplacian. *Numer. Math.*, 142(2):235–278, jun 2019. arXiv:1707.04290, doi:10.1007/s00211-019-01025-x.

[26] Andrea Bonito, Wenyu Lei, and Joseph E Pasciak. On sinc quadrature approximations of fractional powers of regularly accretive operators. *J. Numer. Math.*, 27(2):57–68, jun 2019. arXiv:1709.06619, doi:10.1515/jnma-2017-0116.

[27] Andrea Bonito and Murtazo Nazarov. Numerical Simulations of Surface Quasi-Geostrophic Flows on Periodic Domains. *SIAM J. Sci. Comput.*, 43(2):B405–B430, jan 2021. arXiv:2006.01180, doi:10.1137/20M1342616.

[28] Andrea Bonito and Joseph E Pasciak. Numerical approximation of fractional powers of elliptic operators. *Math. Comput.*, 84(295):2083–2110, mar 2015. arXiv:1307.0888, doi:10.1090/S0025-5718-2015-02937-8.

[29] Andrea Bonito and Peng Wei. Electroconvection of thin liquid crystals: Model reduction and numerical simulations. *J. Comput. Phys.*, 405:109140, mar 2020. doi:10.1016/j.jcp.2019.109140.

[30] Stéphane P.A. Bordas, Sundararajan Natarajan, and Alexander Menk. *Partition of unity methods*. Wiley-blackwell edition, 2016.

[31] Juan Borthagaray, Wenbo Li, and Ricardo H Nochetto. Linear and nonlinear fractional elliptic problems. pages 69–92, jun 2020. arXiv:1906.04230, doi:10.1090/conm/754/15145.

[32] Juan Pablo Borthagaray, Dmitriy Leykekhman, and Ricardo H Nochetto. Local Energy Estimates for the Fractional Laplacian. *SIAM J. Numer. Anal.*, 59(4):1918–1947, jan 2021. arXiv:2005.03786, doi:10.1137/20M1335509.

[33] Raphaël Bulle, Gioacchino Alotta, Gregorio Marchiori, Matteo Berni, Nicola F. Lopomo, Stefano Zaffagnini, Stéphane P. A. Bordas, and Olga Barrera. The Human Meniscus Behaves as a Functionally Graded Fractional Porous Medium under Confined Compression Conditions. *Appl. Sci.*, 11(20):9405, oct 2021. doi:10.3390/app11209405.

[34] Raphaël Bulle, Franz Chouly, Jack S Hale, and Alexei Lozinski. Removing the saturation assumption in Bank–Weiser error estimator analysis in dimension three. *Appl. Math. Lett.*, 107:106429, sep 2020. doi:10.1016/j.aml.2020.106429.

[35] Raphaël Bulle and Jack S Hale. FEniCS Error Estimation (FEniCS-EE), jan 2019. doi:10.6084/m9.figshare.10732421.

[36] Raphaël Bulle, Jack S Hale, Alexei Lozinski, Stéphane P A Bordas, and Franz Chouly. Hierarchical a posteriori error estimation of Bank-Weiser type in the FEniCS Project. feb 2021. URL: http://arxiv.org/abs/2102.04360, arXiv:2102.04360.

[37] Luis Caffarelli and Luis Silvestre. An Extension Problem Related to the Fractional Laplacian. *Commun. Partial Differ. Equations*, 32(8):1245–1260, aug 2007. arXiv:0608640, doi:10.1080/03605300600987306.

[38] Eric Cancès, Geneviève Dusson, Yvon Maday, Benjamin Stamm, and Martin Vohralík. Guaranteed and Robust a Posteriori Bounds for Laplace Eigenvalues and Eigenvectors: Conforming Approximations. *SIAM J. Numer. Anal.*, 55(5):2228–2254, jan 2017. doi:10.1137/15M1038633.

[39] Michele Caputo. Linear Models of Dissipation whose Q is almost Frequency Independent–II. *Geophys. J. Int.*, 13(5):529–539, nov 1967. doi:10.1111/j.1365-246X.1967.tb02303.x.

[40] Michele Caputo. Models of flux in porous media with memory. *Water Resour. Res.*, 36(3):693–705, mar 2000. doi:10.1029/1999WR900299.

[41] Max Carlson, Robert M Kirby, and Hari Sundar. A scalable framework for solving fractional diffusion equations. *Proc. 34th ACM Int. Conf. Supercomput.*, pages 1–11, jun 2020. arXiv:1911.11906, doi:10.1145/3392717.3392769.

[42] Carsten Carstensen and Joscha Gedicke. Guaranteed lower bounds for eigenvalues. *Math. Comput.*, 83(290):2605–2629, apr 2014. doi:10.1090/S0025-5718-2014-02833-0.

[43] Carsten Carstensen and Christian Merdon. Estimator Competition for poisson Problems. *J. Comput. Math.*, 28(3):309–330, 2010. doi:10.4208/jcm.2009.10-m1010.

[44] Huyuan Chen. The Dirichlet elliptic problem involving regional fractional Laplacian. *J. Math. Phys.*, 59(7):071504, jul 2018. arXiv:1509.05838, doi:10.1063/1.5046685.

[45] Long Chen, Ricardo H Nochetto, Enrique Otárola, and Abner J Salgado. A PDE approach to fractional diffusion: A posteriori error analysis. *J. Comput. Phys.*, 293:339–358, jul 2015. doi:10.1016/j.jcp.2015.01.001.

[46] Nicole Cusimano, Félix del Teso, and Luca Gerardo-Giorda. Numerical approximations for fractional elliptic equations via the method of semigroups. *ESAIM Math. Model. Numer. Anal.*, 54(3):751–774, may 2020. doi:10.1051/m2an/2019076.

[47] Nicole Cusimano, Félix del Teso, Luca Gerardo-Giorda, and Gianni Pagnini. Discretizations of the Spectral Fractional Laplacian on General Domains with Dirichlet, Neumann, and Robin Boundary Conditions. *SIAM J. Numer. Anal.*, pages 1243–1272, jan 2018. arXiv:1708.03602, doi:10.1137/17M1128010.

[48] Tobias Danczul and Joachim Schöberl. A Reduced Basis Method For Fractional Diffusion Operators I. pages 1–19, 2019. URL: http://arxiv.org/abs/1904.05599, arXiv:1904.05599.

[49] Tobias Danczul and Joachim Schöberl. A reduced basis method for fractional diffusion operators II. *J. Numer. Math.*, 29(4):269–287, oct 2021. arXiv:2005.03574, doi:10.1515/jnma-2020-0042.

[50] Ozlem Defterli, Marta D'Elia, Qiang Du, Max Gunzburger, Rich Lehoucq, and Mark M Meerschaert. Fractional Diffusion on Bounded Domains. *Fract. Calc. Appl. Anal.*, pages 1689–1699, jan 2015. arXiv:arXiv:1011.1669v3, doi:10.1515/fca-2015-0023.

[51] Marta D'Elia and Max Gunzburger. The fractional Laplacian operator on bounded domains as a special case of the nonlocal diffusion operator. *Comput. Math. with Appl.*, pages 1245–1260, oct 2013. arXiv:1303.6934, doi:10.1016/j.camwa.2013.07.022.

[52] Huy Dinh, Harbir Antil, Yanlai Chen, Elena Cherkaev, and Akil Narayan. Model reduction for fractional elliptic problems using Kato's formula. *Math. Control Relat. Fields*, 2021. doi:10.3934/mcrf.2021004.

[53] Willy Dörfler. A Convergent Adaptive Algorithm for Poisson's Equation. *SIAM J. Numer. Anal.*, 33(3):1106–1124, jun 1996. doi:10.1137/0733054.

[54] Qiang Du, Jiang Yang, and Zhi Zhou. Time-Fractional Allen–Cahn Equations: Analysis and Numerical Methods. *J. Sci. Comput.*, page 42, nov 2020. arXiv:1906.06584, doi:10.1007/s10915-020-01351-5.

[55] Siwei Duo, Hong Wang, and Yanzhi Zhang. A comparative study on nonlocal diffusion operators related to the fractional Laplacian. *Discret. Contin. Dyn. Syst. - B*, pages 231–256, 2019. arXiv:1711.06916, doi:10.3934/dcdsb.2018110.

[56] Robert D Falgout and Ulrike Meier Yang. hypre: A Library of High Performance Preconditioners. In Peter M A Sloot, Alfons G Hoekstra, C J Kenneth Tan, and Jack J Dongarra, editors, *Comput. Science — ICCS 2002*, number 2331 in Lecture Notes in Computer Science, pages 632–641. Springer Berlin Heidelberg, apr 2002. doi:10.1007/3-540-47789-6_66.

[57] Mouhamed M Fall. Regional fractional Laplacians: Boundary regularity. *arXiv*, jul 2020. URL: http://arxiv.org/abs/2007.04808, arXiv:2007.04808.

[58] Markus Faustmann, Michael Karkulik, and Jens M Melenk. Local convergence of the FEM for the integral fractional Laplacian. *arXiv*, pages 1–20, may 2020. URL: http://arxiv.org/abs/2005.14109, arXiv:2005.14109.

[59] Markus Faustmann, Jens M Melenk, and Dirk Praetorius. Quasi-optimal convergence rate for an adaptive method for the integral fractional Laplacian. *Math. Comput.*, 90(330):1557–1587, apr 2021. arXiv:1903.10409, doi:10.1090/mcom/3603.

[60] Ivan P Gavrilyuk, Wolfgang Hackbusch, and Boris N Khoromskij. Data-sparse approximation to the operator-valued functions of elliptic operator. *Math. Comput.*, pages 1297–1325, jul 2003. doi:10.1090/S0025-5718-03-01590-4.

[61] Ivan P Gavrilyuk, Wolfgang Hackbusch, and Boris N Khoromskij. Data-sparse approximation to a class of operator-valued functions. *Math. Comput.*, pages 681–709, aug 2004. doi:10.1090/S0025-5718-04-01703-X.

[62] Heiko Gimperlein and Jakub Stocek. Space–time adaptive finite elements for nonlocal parabolic variational inequalities. *Comput. Methods Appl. Mech. Eng.*, pages 137–171, aug 2019. arXiv:1810.06888, doi:10.1016/j.cma.2019.04.019.

[63] Gerd Grubb. Fractional Laplacians on domains, a development of Hörmander's theory of μ-transmission pseudodifferential operators. *Adv. Math. (N. Y).*, 268:478–528, jan 2015. doi:10.1016/j.aim.2014.09.018.

[64] Michal Habera, Jack S Hale, Chris Richardson, Johannes Ring, Marie Rognes, Nate Sime, and Garth N Wells. FEniCSX: A sustainable future for the FEniCS Project. 2020. doi:10.6084/m9.figshare.11866101.v1.

[65] Jack S. Hale, Lizao Li, Christopher N. Richardson, and Garth N. Wells. Containers for Portable, Productive, and Performant Scientific Computing. *Computing in Science & Engineering*, 19(6):40–50, November 2017. doi:10.1109/MCSE.2017.2421459.

[66] Stanislav Harizanov, Svetozar Margenov, and Nedyu Popivanov. Spectral Fractional Laplacian with Inhomogeneous Dirichlet Data: Questions, Problems, Solutions. pages 123–138, 2021. arXiv:arXiv:2010.01383v1, doi:10.1007/978-3-030-71616-5_13.

[67] Nicholas J. Higham and Lijing Lin. An Improved Schur–Padé Algorithm for Fractional Powers of a Matrix and Their Fréchet Derivatives. *SIAM J. Matrix Anal. Appl.*, 34(3):1341–1360, jan 2013. doi:10.1137/130906118.

[68] Clemens Hofreither. A unified view of some numerical methods for fractional diffusion. *Comput. Math. with Appl.*, 80(2):332–350, jul 2020. doi:10.1016/j.camwa.2019.07.025.

[69] Clemens Hofreither. An algorithm for best rational approximation based on barycentric rational interpolation. *Numer. Algorithms*, 88(1):365–388, sep 2021. doi:10.1007/s11075-020-01042-0.

[70] Mateusz Kwaśnicki. Ten equivalent definitions of the fractional laplace operator. *Fract. Calc. Appl. Anal.*, 20(1):7–51, jan 2017. arXiv:1507.07356, doi:10.1515/fca-2017-0002.

[71] Finn Lindgren, Håvard Rue, and Johan Lindström. An explicit link between Gaussian fields and Gaussian Markov random fields: the stochastic partial differential equation approach. *J. R. Stat. Soc. Ser. B (Statistical Methodol.)*, 73(4):423–498, sep 2011. doi:10.1111/j.1467-9868.2011.00777.x.

[72] Anna Lischke, Guofei Pang, Mamikon Gulian, Fangying Song, Christian Glusa, Xiaoning Zheng, Zhiping Mao, Wei Cai, Mark M Meerschaert, Mark Ainsworth, and George Em Karniadakis. What is the fractional Laplacian? A comparative review with new results. *J. Comput. Phys.*, 404:109009, mar 2020. arXiv:1801.09767, doi:10.1016/j.jcp.2019.109009.

[73] Dominik Meidner, Johannes Pfefferer, Klemens Schürholz, and Boris Vexler. *hp*-Finite Elements for Fractional Diffusion. *SIAM J. Numer. Anal.*, 56(4):2345–2374, jan 2018. arXiv:1706.04066, doi:10.1137/17M1135517.

[74] Chenchen Mou and Yingfei Yi. Interior Regularity for Regional Fractional Laplacian. *Commun. Math. Phys.*, 340(1):233–251, nov 2015. doi:10.1007/s00220-015-2445-2.

[75] Ricardo H Nochetto, Enrique Otárola, and Abner J Salgado. A PDE Approach to Fractional Diffusion in General Domains: A Priori Error Analysis. *Found. Comput. Math.*, 15(3):733–791, jun 2015. arXiv:1302.0698, doi:10.1007/s10208-014-9208-x.

[76] Ricardo H Nochetto, Tobias von Petersdorff, and Chen-Song Zhang. A posteriori error analysis for a class of integral equations and variational inequalities. *Numer. Math.*, 116(3):519–552, sep 2010. doi:10.1007/s00211-010-0310-y.

[77] Angel Plaza and Graham F Carey. Local refinement of simplicial grids based on the skeleton. *Appl. Numer. Math.*, 32(2):195–218, feb 2000. doi:10.1016/S0168-9274(99)00022-7.

[78] Igor Podlubny, Aleksei Chechkin, Tomas Skovranek, YangQuan Chen, and Blas M. Vinagre Jara. Matrix approach to discrete fractional calculus II: Partial fractional differential equations. *J. Comput. Phys.*, 228(8):3137–3153, may 2009. doi:10.1016/j.jcp.2009.01.014.

[79] Pablo Raúl Stinga. User's guide to the fractional Laplacian and the method of semigroups. In *Fract. Differ. Equations*, pages 235–266. De Gruyter, feb 2019. arXiv:1808.05159, doi:10.1515/9783110571660-012.

[80] Pablo Raúl Stinga and José Luis Torrea. Extension Problem and Harnack's Inequality for Some Fractional Operators. *Commun. Partial Differ. Equations*, 35(11):2092–2122, oct 2010. arXiv:0910.2569, doi:10.1080/03605301003735680.

[81] Petr N Vabishchevich. Approximation of a fractional power of an elliptic operator. *Numer. Linear Algebr. with Appl.*, 27(3):1–17, may 2020. arXiv:1905.10838, doi:10.1002/nla.2287.

[82] Rüdiger Verfürth. Robust a posteriori error estimators for a singularly perturbed reaction-diffusion equation. *Numer. Math.*, 78(3):479–493, jan 1998. doi:10.1007/s002110050322.

[83] Christian J Weiss, Bart G van Bloemen Waanders, and Habir Antil. Fractional Operators Applied to Geophysical Electromagnetics. *Geophys. J. Int.*, pages 1242–1259, nov 2019. arXiv:1902.05096, doi:10.1093/gji/ggz516.

[84] Xuan Zhao, Xiaozhe Hu, Wei Cai, and George Em Karniadakis. Adaptive finite element method for fractional differential equations using hierarchical matrices. *Comput. Methods Appl. Mech. Eng.*, 325:56–76, oct 2017. arXiv:1603.01358, doi:10.1016/j.cma.2017.06.017.

Centro de Investigación en Ingeniería Matemática (CI^{2}MA)

PRE-PUBLICACIONES 2022

2022-09 Julio Aracena, Florian Bridoux, Luis Gomez, Lilian Salinas: *Complexity of limit cycles with block-sequential update schedules in conjunctive networks*

2022-10 Eligio Colmenares, Gabriel N. Gatica, Juan Carlos Rojas: *A Banach spaces-based mixed-primal finite element method for the coupling of Brinkman flow and nonlinear transport*

2022-11 Sergio Caucao, Gabriel N. Gatica, Ricardo Oyarzúa, Paulo Zuñiga: *A posteriori error analysis of a mixed finite element method for the coupled Brinkman–Forchheimer and double-diffusion equations*

2022-12 Sergio Caucao, Gabriel N. Gatica, Juan P. Ortega: *A posteriori error analysis of a Banach spaces-based fully mixed FEM for double-diffusive convection in a fluid-saturated porous medium*

2022-13 Raimund Bürger, Julio Careaga, Stefan Diehl, Romel Pineda: *A model of reactive settling of activated sludge: comparison with experimental data*

2022-14 Gabriel N. Gatica, Nicolas Nuñez, Ricardo Ruiz-Baier: *New non-augmented mixed finite element methods for the Navier-Stokes-Brinkman equations using Banach spaces*

2022-15 Dibyendu Adak, David Mora, Alberth Silgado: *A Morley-type virtual element approximation for a wind-driven ocean circulation model on polygonal meshes*

2022-16 Sergio Caucao, Eligio Colmenares, Gabriel N. Gatica, Cristian Inzunza: *A Banach spaces-based fully-mixed finite element method for the stationary chemotaxis-Navier-Stokes problem*

2022-17 Felipe Lepe, David Mora, Gonzalo Rivera, Iván Velásquez: *A posteriori virtual element method for the acoustic vibration problem*

2022-18 Franz Chouly: *A review on some discrete variational techniques for the approximation of essential boundary conditions*

2022-19 Veronica Anaya, Ruben Caraballo, Sergio Caucao, Luis F. Gatica, Ricardo Ruiz-Baier, Ivan Yotov: *A vorticity-based mixed formulation for the unsteady Brinkman-Forchheimer equations*

2022-20 Olga Barrera, Stéphane P. A. Bordas, Raphaël Bulle, Franz Chouly, Jack S. Hale: *An a posteriori error estimator for the spectral fractional power of the Laplacian*

Para obtener copias de las Pre-Publicaciones, escribir o llamar a: Director, Centro de Investigación en Ingeniería Matemática, Universidad de Concepción, Casilla 160-C, Concepción, Chile, Tel.: 41-2661324, o bien, visitar la página web del centro: `http://www.ci2ma.udec.cl`







Centro de Investigación en
Ingeniería Matemática (CI²MA)
Universidad de Concepción

Casilla 160-C, Concepción, Chile
Tel.: 56-41-2661324/2661554/2661316
http://www.ci2ma.udec.cl